Objectives of Report

This report describes the structural behavior of the Harshman Bridge, built in 1894 by Everett S. Sherman over Four Mile Creek in Preble County, Ohio. The basic form of this bridge resembles the Childs truss, patented in 1846 by Horace Childs. The Childs truss utilizes both wooden and wrought iron members in its form, but unlike other wood and iron truss types, such as the Howe or Pratt, the Childs truss does not involve prestressing in its design. The main objective of this report was to quantify the behavior of the Harshman Bridge through physical experiments and dead load, live load, and creep analyses. Another objective was to compare the Childs truss form to its contemporary truss types, Long, Howe, and Pratt.

Scope of Work

Physical experiments on the bridge, including tightening of a tension rod and load tests with a 12-ton truck, were conducted in order to assess the behavior of the Harshman Bridge and compare results with analytical studies of the bridge. Plane truss and plane frame models were used for the dead load analyses and one live load analysis to compare the results of manual versus computer structural analyses. This was done mainly to determine how close the manually calculated plane truss models, which existed at the time Sherman constructed his bridges, correspond to the computer analyses. Live loads considered include a unit load at midspan, a unit load traversing the length of the truss, and a uniform live load over half-span and over full span. A tightening analysis was performed to assess the effects of tightening the nuts after the dead load was active. The effects of time-dependent behavior of wood on the Harshman Bridge were also studied.

Observations

Two physical experiments were conducted on the Harshman Bridge. Test 1 was simply the loosening and tightening of tension rod U_0L_1, which was intended to model the physical tightening of the rods during construction. Manual tightening produced an axial force of 2300 lbs. Test 2 involved traversing the bridge with a 12-ton truck. Three runs were made, and the results were compared with the various analyses of the bridge.

For the dead load analyses, manually calculated stresses in a plane truss model were compared to the computer-calculated stresses in a plane frame model. Results from the two analyses were similar, with maximum forces of over 50 kips for both the top and bottom chord, about 10 kips for the verticals, about 23 kips for the compression diagonals, and 9.3 kips for the tension rods. The ratio of vertical components of forces in the diagonal members of the plane truss model was assumed to be proportional to the axial stiffnesses of the members. This underestimated the force taken by the tension rods as predicted by the plane frame analysis. The contributions of bending moments to the maximum normal stress in the elements were calculated, resulting in contributions between 10 and 40 percent of the total stress. The vertical midspan displacements predicted with the two models were 0.834” for the plane truss and 0.773” for the plane frame, which shows the contributions of member bending stiffness to the bridge stiffness.

Both plane truss and plane frame models were used to analyze a live load condition of a unit vertical force at midspan, again to compare the predictions of both models. Results yielded correspondence similar to that of the dead load analyses. The ratio of vertical components of force in the diagonal elements was again assumed to be proportional to the axial stiffnesses of the elements for the plane truss model. This underestimated the axial force in the tension rods as predicted by the plane frame analyses. The contributions of bending moments to element stresses in the plane frame model were determined to range between 20 and 60 percent. The vertical midspan displacement of the plane truss model, 0.0308", was again higher than that determined by the plane frame model, 0.0209", because bending stiffness was considered in the latter.

A vertical unit load was placed on each panel point along the bottom truss to generate influence lines for axial forces in various truss elements and also for comparison with the results of the load tests. The influence lines successfully predict trends in the element forces, but the measured forces do not always correspond. Maximum forces from the passage of the 12-ton truck were 1 kip tension in vertical U_4L_4, 6 kips compression in compressive diagonal U_3L_2, and 4 kips tension in tensile diagonals U_1L_2 and U_3L_4. The average displacement for the east and west truss due to the 12 ton load was 0.27".

A typical nineteenth century design live load of 80 lbs/ft^2 was placed over half the span and the full span of the Harshman Bridge to check performance under these conditions. Maximum stresses when the load was placed over the entire span were all within or below the acceptable range of allowable bending stress in pine and wrought iron. With the live load over half the span, looseness was predicted in one compression diagonal. The minimum loads to cause looseness in the compression diagonals adjacent to the midspan were predicted to be a uniform live load of 57 lbs/ft^2 over half the span or a concentrated vertical load of 9.5 kips at node L_5. Stresses were checked in the girders with and without the retrofitted steel beams. The steel beams increase the maximum shear stress by 8 percent, but reduce the normal stress in the girders by 85 percent.

Tightening of the truss with dead load active was also modeled. Tightening caused an increase of tension in the rods, a decrease in the compressive forces in the wood diagonals, and a decrease of tension in the verticals. Members in panels adjacent to the tightened rod experienced significantly smaller forces, and the tightening caused very small displacements.

A creep analysis was performed using the plane frame model and assuming a strain due to creep of ±0.0005. For a truly accurate calculation of stresses and displacements due to creep, viscoelastic analyses would be required, but this approximate analysis shows the general redistribution of member forces due to creep of the wood.

The Long, Howe, and Pratt prestressed trusses were in use at the time of the Childs truss patent. The novelty of the Childs truss in comparison with these other forms was that it did not need to be prestressed in order for both its diagonals to be active.

Early Wood Truss Bridges and the Horace Childs Patent of August 1846

Timothy Palmer built the first covered bridge in the United States in 1805 in Philadelphia over the Schuylkill River. Desiring to prevent the weathering common to wooden truss bridges at the time, Palmer added a roof and exterior walls to his arch truss to dramatically increase its life.[1] Other early covered bridge builders were Theodore Burr, Lewis Wernwag, and Ithiel Town. Burr employed the kingpost truss and combined it with an arch for his patent of April 1817.[2] Lewis Wernwag built his Colossus Bridge over the Schuylkill River in 1812. It was constructed of five parallel arched trusses, and spanned over 340'.[3] Ithiel Town received a patent for his lattice truss design in January of 1820. With its many over-lapping wood planks and drilled connections at each intersection with hardwood pegs (trunnels), Town's design was very rigid.[4]

In 1826, C. Navier published a set of lectures that included analysis and design techniques for simple trusses. Navier gave solutions for finding forces in a simple triangular truss, and a method for finding forces in simple statically indeterminate trusses. He also introduced the concept of analyzing a parallel chord truss as a beam, where the stiffness of the truss is proportional to the chord areas times the square of the distance between the chords. Navier's developments were used by American truss bridge designers in the 1830s and 1840s.[5]

Stephen Long received a patent for a truss in March 1830. Long introduced prestressing to wooden truss bridges and used Navier's developments to design trusses possessing a known flexural strength.[6] His design consisted of two parallel chords divided into panels, with each panel consisting of a main diagonal brace and a counter brace, which were both placed into compression by wedges driven between the counter and the chords. Prestressing avoided the need for tension connections in the braces, allowed the diagonals to add to the stiffness of the truss, permitted some shrinkage in the wood, and provided camber to the bridge.[7]

William Howe's second truss bridge patent, granted in August 1840, offered a new method of prestressing. Howe replaced the vertical posts with iron rods that could be

---

[1] *American Wooden Bridges*, (New York: American Society of Civil Engineers Historical Publication, 1976).
[2] *Engineering News and American Contract Journal* (October 28, 1882), p. 371
[3] *American Wooden Bridges*.
[4] The influence of the Town lattice truss design in both the United States and Europe has been examined in G.K. Dreicer, "The Long Span. Intercultural Exchange in Building Technology," (Ph.D. diss., Cornell University, Ithaca, New York, 1993).
[5] D.A. Gasparini and C. Provost, "Early Nineteenth Century Developments in Truss Design in Britain, France, and the United States," *Journal of the Construction History Society* 5 (1989): p. 22.
[6] D.A. Gasparini and C. Simmons, "American Truss Bridge Connections in the 19th Century, Part I: 1829-1850," *American Society of Civil Engineers Journal of Performance of Constructed Facilities* II, no. 3 (August 1997): p. 119.
[7] Gasparini and Provost, "Early Nineteenth Century Developments in Truss Design," p. 28.

tightened.[8] His patented double-intersection form was later revised to have a single-intersection in the diagonal members. The truss was prestressed by tightening nuts at the top chord, making the Howe truss easier to construct than the Long. Because of this ease of construction, the uniformity in member sizes, and ability to easily replace and repair parts of the truss, railroad companies extensively utilized Howe's design.[9]

In April 1844, Thomas and Caleb Pratt received a patent for their truss. Like Howe, they introduced threaded iron rods into their truss for use as prestressing elements. These iron main diagonals and counter diagonals extended through the top and bottom chords, where they were fastened with nuts and could be tightened. The important difference between the Pratt truss and the Howe truss was that the system of two iron tension elements per panel allows for greater control of the camber in the bridge and the tensile iron diagonals make the Pratt form more efficient.[10] However, the inclined tension elements were more difficult to pretension and caused compression perpendicular to the grain of the wood chords.

Horace Childs, a nephew of S.H. Long, had first-hand experience with construction of the Long truss.[11] Childs was a sub-agent for the Long truss patent, which means he had acquired the right to use the Long truss for any bridge he might erect. He is known to have supervised the construction of at least one Long truss bridge–a two-span, 340' long structure crossing the Connecticut River at Haverhill, New Hampshire.[12]

Horace Childs conceived his own truss form and received a patent on August 12, 1846 (Figure 1). Childs hoped to correct certain "defects" in wooden truss bridges. Childs' main concerns with truss bridges such as Long's were the high levels of tensile stress in the vertical posts and the lack of positive connections between the diagonal members and the chords and posts.[13]

---

[8] *Engineering News and American Contract Journal* (November 11, 1882), p. 394.
[9] Gasparini and Simmons, "American Truss Bridges in the 19th Century. Part I," p. 123.
[10] *Engineering News and American Contract Journal* (December 2, 1882), p. 418;
Gasparini and Simmons, "American Truss Bridge Connections in the 19th Century. Part I," p. 126.
[11] Geneological Records, New Hampshire Antiquarian Society, 300 Main Street, Hopkinton, NH.
[12] S.H. Long, *Description of Col. Long's Bridges together with a Series of Directions to Bridge Builders* (Concord, NH: Start and Universalist Press, 1836), pp. 47-48.
[13] H. Childs, Patent No. 4693, August 12, 1846.

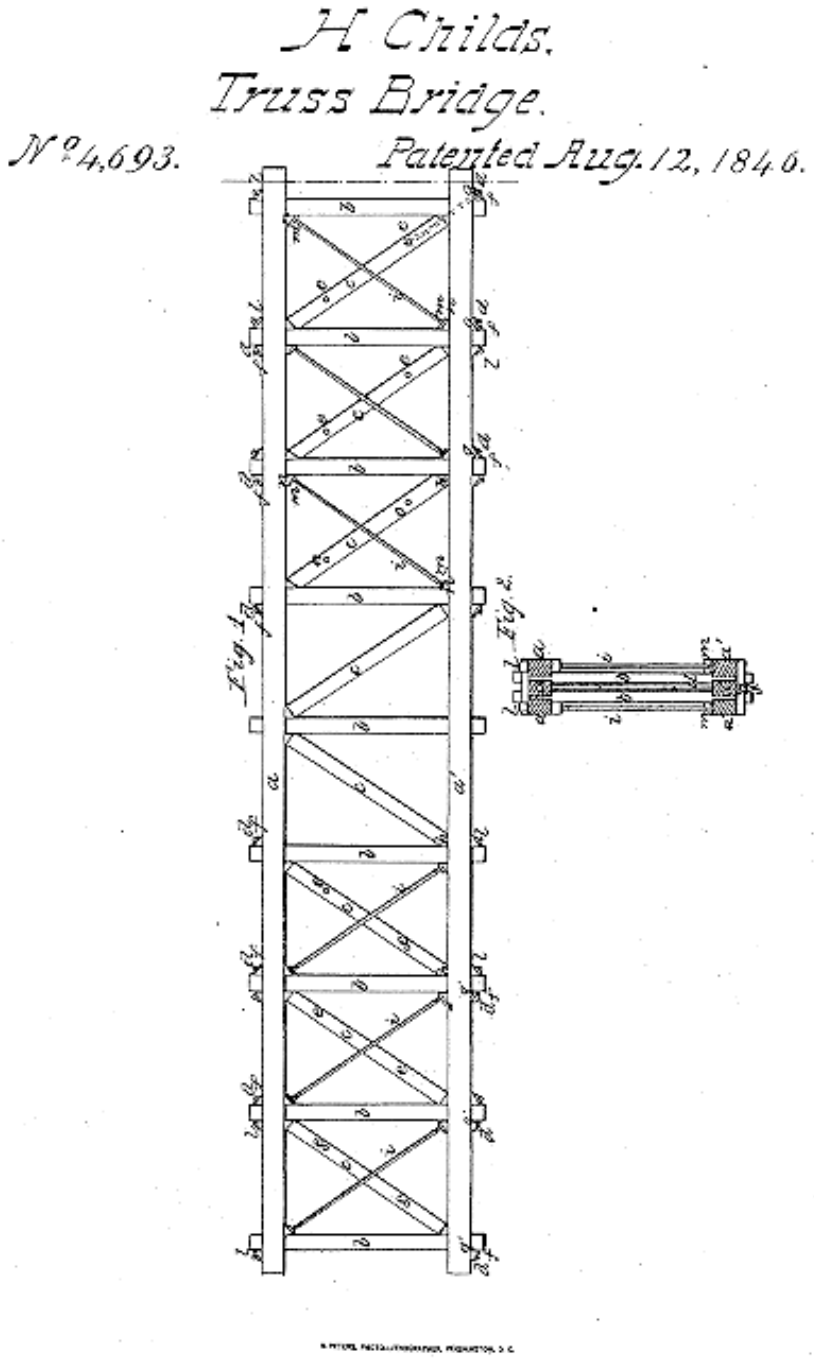

Figure 1. Childs truss, Patent No. 4693, August 12, 1846

Childs made only two claims in his patent, both of which involved new connection details for the diagonal members. The first idea was the addition of nuts and "shoe pieces" to the suspension rods at the underside of the top chord and the upper side of the

bottom chord. This modification was intended to secure the connection between the posts and the chords. Secondly, Childs suggested adding a mechanical connection to the compressive diagonals by way of a screw bolt, secured by a pin through the diagonals and the eye of the bolt, and extending the screw bolt through the chord and post where it could be secured on the outside with a nut, as shown in Figure 2.[14] Both of these features are described in the patent but they are barely visible in Childs' patent drawing.

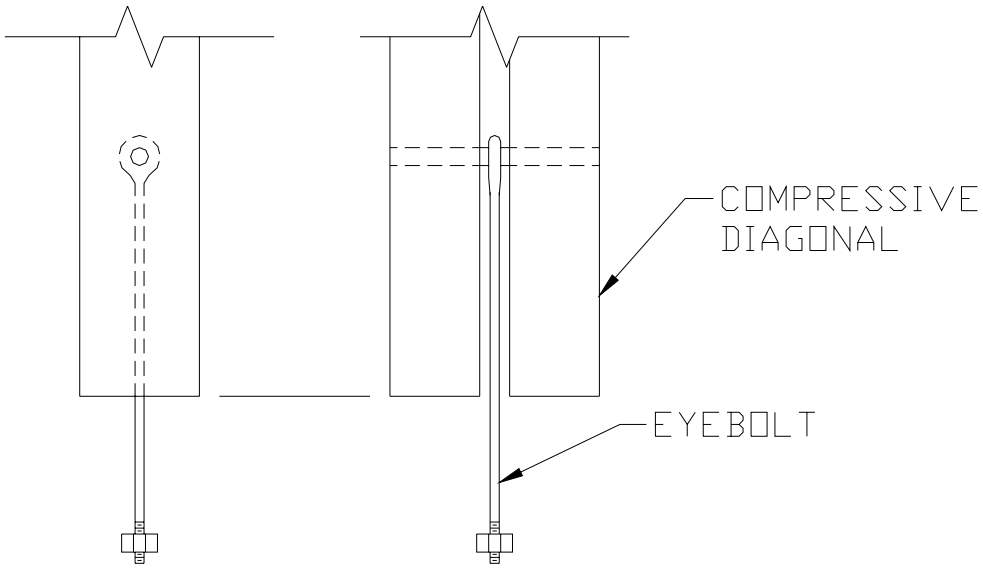

Figure 2. Detail of eyebolt connection detail patented by Childs

The motive behind Childs' decision to patent his diagonal brace connections is unknown, but it may have been intended to make construction of the bridge truss easier by providing threaded bolt connections for both diagonals, unlike the simple bearing connections of a Long truss. Aside from constructability issues, one definite advantage of Childs' truss design over that of Long's was that the tensile forces in the vertical posts were less with the counter diagonals in tension. The transfer of large tensile forces into the verticals in a Long truss can lead to shear failures in the wood "shoulders" of the verticals, such as the Eldean Bridge (see HAER No. OH-122).

A peculiar feature of Childs' design is that the center panels of the truss lack mechanical connections in the compressive diagonals and suspension/counter braces. The absence of these can lead to the central diagonals becoming loose under heavy live loads near mid span. Childs' reasons for this feature are unknown (they are never mentioned in the

[14] Childs, Patent No. 4693, August 12, 1846.

patent), but perhaps he saw it as a way to simplify the bridge or make it more economical.
Assuming that the eyebar detail shown in Figure 2 could not develop significant tension, the Childs truss could not be prestressed in the same way as the Long, Howe and Pratt forms. The primary effect of tightening the nuts on the counters was to provide camber and decrease the dead load compressive forces in the main diagonals.

Everett Sherman and the Harshman Bridge

Everett Sherman built the Chambers Road Bridge over Big Walnut Creek in Delaware County, Ohio, in 1883 (see Figure 3). The bridge is comprised of eight panels, and it has wooden compression and wrought iron tension diagonals, except in the innermost panels, which have only wood compression members. The top chords have simple butt joints, the wood diagonals rely on compression for their connections, and the tension rods are secured with nuts only on the outside of the chords.

Figure 3. Chambers Road Bridge, built by Everett Sherman in 1883

There is evidence of many repairs to the Chambers Road Bridge, likely in response to deterioration of the bridge. Some of the butt joints in the top chord have shifted (perhaps when the midspan pier was added), making them ineffective, and they were haphazardly nailed back together at an unknown time (Figure 4). In places, pieces of wood have been wedged in between the top of the compressive diagonals and the intersection of the verticals and chords (Figure 5), most likely to introduce some compression to the

members and help them stay in place. There are two vertical steel rods on either side of the vertical posts (Figure 5). These may have been part of the original design or a retrofit. One of the vertical rods passes through the bottom chord and carries a section of the girder, thus it transfers part of the floor loads directly to the top nodes. The other vertical rod may have been intended to decrease or eliminate any potential tensile force in the vertical. More significantly, a central pier and longitudinal steel beams were added to the Chambers Road Bridge. These retrofits changed or eliminated the structural role of the trusses.

The Chambers Road Bridge does not have two details of the Childs truss patent, that is, two nuts at each end of the diagonal rods and the eyebolts. It resembles the Childs truss in the use of a combination of wood and iron diagonals and the omission of iron diagonals in the panels adjacent to the midspan.

Figure 4. Chambers Road Bridge, detail of butt joint

Figure 5. Chambers Road Bridge, detail of connection

In the late 1880s, Sherman moved to Preble County, Ohio, because of an invitation from county engineer Robert Eaton Lowery to rebuild county bridges destroyed by a storm in May 1887. Between 1887 and 1895, Sherman constructed fifteen bridges similar in design to the Chambers Road Bridge and echoing the form of the Childs truss.[15]

The Harshman Bridge

Sherman constructed the Harshman Bridge over Four Mile Creek in Preble County in 1894. Spanning 109', this bridge is of the same basic form as Sherman's others in Preble County. It is a skew bridge, with dummy panels added to provide square end portals, as shown in Figure 6. The bridge is about 18' tall from the ground to peak of the roof and is only wide enough for one vehicle. The wood species used on the Harshman Bridge have not been determined, but it is likely that the superstructure is pine and the floor is oak. The posted load limit is 12 tons.

[15] Wood, *The Covered Bridges of Ohio*, pp. 29-30

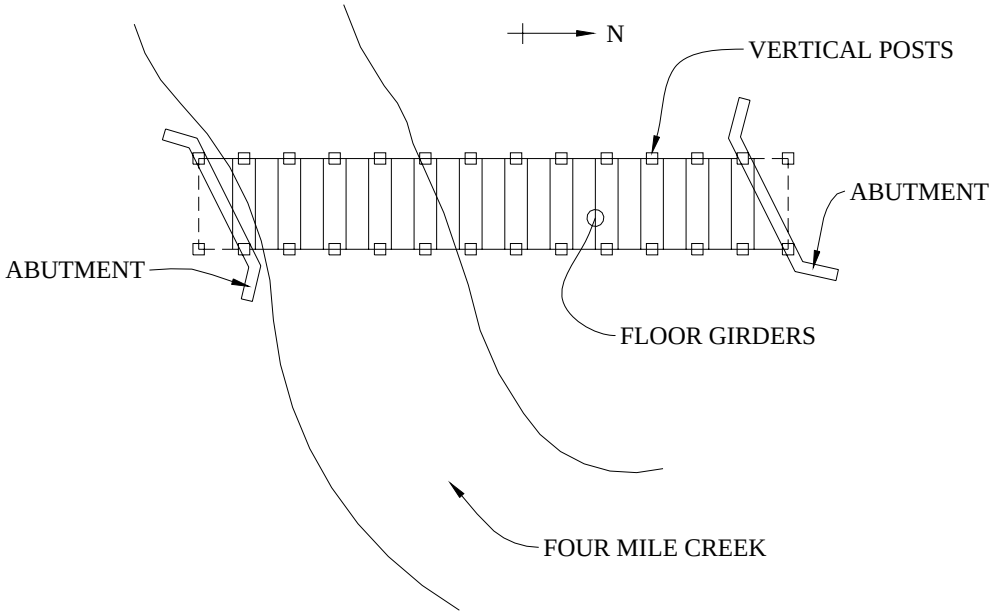

Figure 6. Skew of Harshman Bridge relative to Four Mile Creek

Like the Chambers Road Bridge, the Harshman bridge consists of wooden compression members sans positive connections; iron diagonals secured with nuts only on the outside of the chords; butt joints along the top chord; and both bolt and trunnel connections along the bottom chord (Figure 7). The spacing of the girders is approximately half the panel width. They are attached by U-bolts (Figures 8, 9) to the bottom chord. The connection on the left of Figure 8, made of wood blocks and square nuts, is probably an original detail, while the right connection is a retrofit.

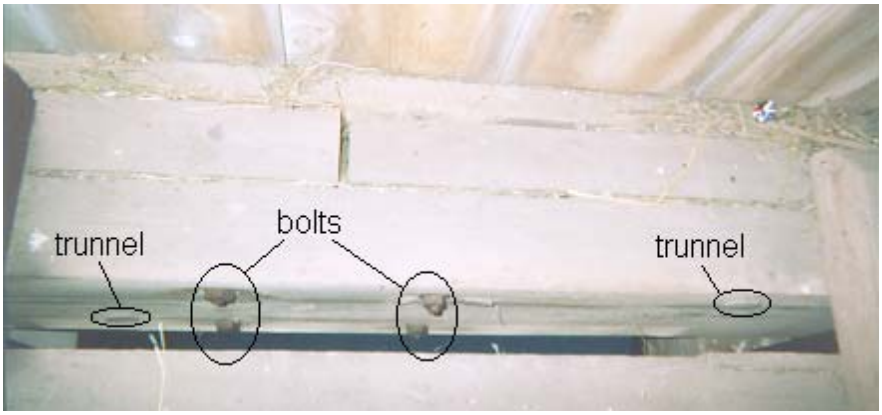

Figure 7. Bottom chord splice detail

Figure 8. Detail of U-bolt connection of girders to the bottom chord (older connection on left)

Figure 9. Underside of U-bolt connection showing the retrofitted steel beams

The framing provides lateral stiffness (shown in Figure 10), which exists at every panel point.

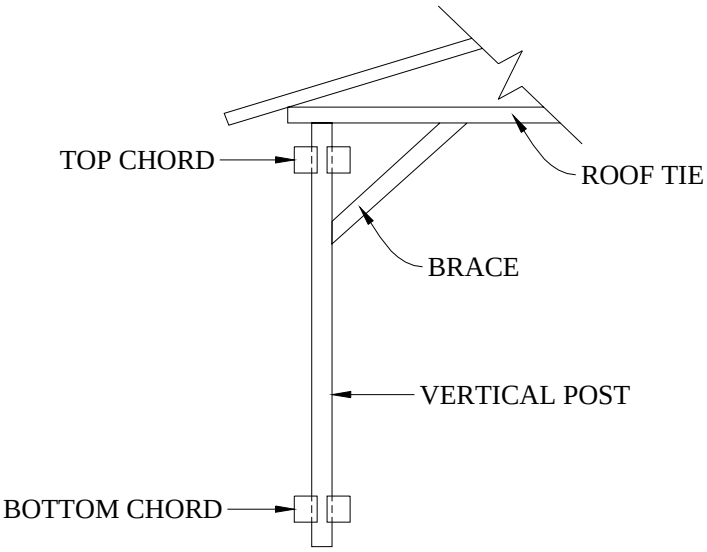

Figure 10. Lateral bracing system

One interesting feature of the bridge is the sizing of the wooden compressive diagonals and iron tensile diagonals. Starting at the outermost panel and working towards the center, each panel contains a compressive diagonal of slightly smaller thickness, varying from 7.5" to 2.5" at the center panel. The suspension rods vary similarly, from 1.25" to 1" closest to the center.

Despite its age, the Harshman Bridge appears to be in excellent condition and has only seen some minor repairs. The approaches are well graded. Insect damage (a hole approximately 6" long and 1.5" wide) exists on the east end of the northernmost girder. Steel beams have been attached to the bottom of the girders. These help the wood girders in bending only. The compression diagonal in the south panel adjacent to the centerline of the east truss is loose and out of plane. Like the Chambers Road Bridge, the chords are only connected with butt joints, which appear to be in good condition. Bolts and trunnels connect the bottom chords. The roof of the bridge was not inspected.

Probably the most significant modifications to the Harshman Bridge were done near the supports. Short lengths of the bottom chords at each end of the bridge have been replaced and spliced with steel plates. The bottom halves of the vertical posts that connect into these chords have also been replaced. Concrete bearing pads, 5" thick, have been added at the four support points. The piers have been treated with unite, likely to protect against further freeze-thaw damage in the stone. No evidence of scouring is evident on the piers, and under normal flow conditions, the northern pier is in dry conditions.

There were many differences between Sherman's design of the Harshman Bridge and Childs' patent truss. Sherman used a single compressive diagonal and a single rod passing through a hole in the wood, whereas Childs' patent called for pairs of iron and wood pieces for the diagonals. Another important difference is the absence of the eyebolt connection in the compressive diagonals and the extra nuts on the tensile rods, both of the patented features of Childs' design. Therefore it may more precisely be said that the Harshman Bridge is of a design particular to Everett Sherman; it only resembles the patented Childs truss in its use of wrought iron rods for the tension diagonals and wood for the compressive diagonals. Simmons hypothesizes that Sherman saw an 1882 *Engineering News* article on expired bridge truss patents and that he adapted the Childs truss for all his designs, beginning with the Chambers Road Bridge.[16]

There are interesting questions and issues related to the design, construction, and behavior of the Harshman Bridge. The bridge was designed in 1894, when statically determinate analyses were well-known and statically determinate truss forms dominated. How did Sherman analyze the bridge, and proportion the size of the diagonals? Why did Sherman use closely-spaced girders, which produce bending in the lower chords? How were the nuts tightened? As constructed, how did the bridge carry dead loads and live loads and what were the effects of wood creep on the structural behavior? To study these issues, the bridge was tested and analyzed as follows.

Testing of the Harshman Bridge

The Harshman Bridge was instrumented and tests were performed to determine its structural behavior. Strain gauges and strain transducers were placed on the southern half of the west truss. Five strain gauges were used, one on each tension rod, and eight strain transducers were used on wooden members, six on compression diagonals and two on a vertical post. The instruments were positioned as shown in Figure 11.

[16] David A. Simmons, "Unique Covered Bridges in Delaware County" *Ohio County Engineering News* (Spring 1991), p. 10; *Engineering News and American Contract Journal* (December 16, 1882), p. 433.

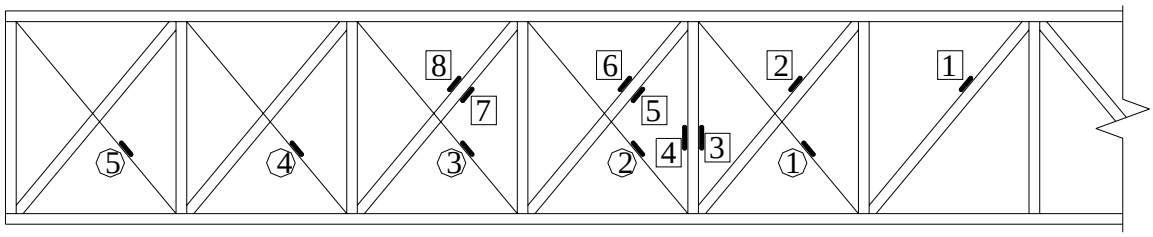

◯ = ELECTRICAL RESISTANCE STRAIN GAUGE

□ = STRAIN TRANSDUCER

Figure 11. Placement of instruments

Figure 12 shows a typical strain transducer attached to the timber diagonal with two 1/4" lag screws. In addition, displacement transducers (DCDTs) were placed at the midspans of both trusses to measure the vertical deflection of the bridge during tests (Figure 13).

Figure 12. Strain transducer on compression diagonal

Figure 13. Displacement transducers to measure vertical deflection

The first test performed on the bridge consisted of loosening and tightening the top nut of the southernmost tension diagonal on the west truss. Figure 14 shows that the axial force in the bar reached a maximum value over 2300 pounds. In a 2002 study of the Pine Bluff Bridge (see HAER No. IN-103), a Howe truss in Putnam County, Indiana, a similar experiment (with the same person tightening the nut using the same wrench) yielded a maximum force of over 6000 pounds. Results of such experiments are very dependent on the amount of rust present, the pitch of the treads, and probably the diameter of the rod, but they are nonetheless useful for providing data on the tension that can be induced by manually tightening a nut.

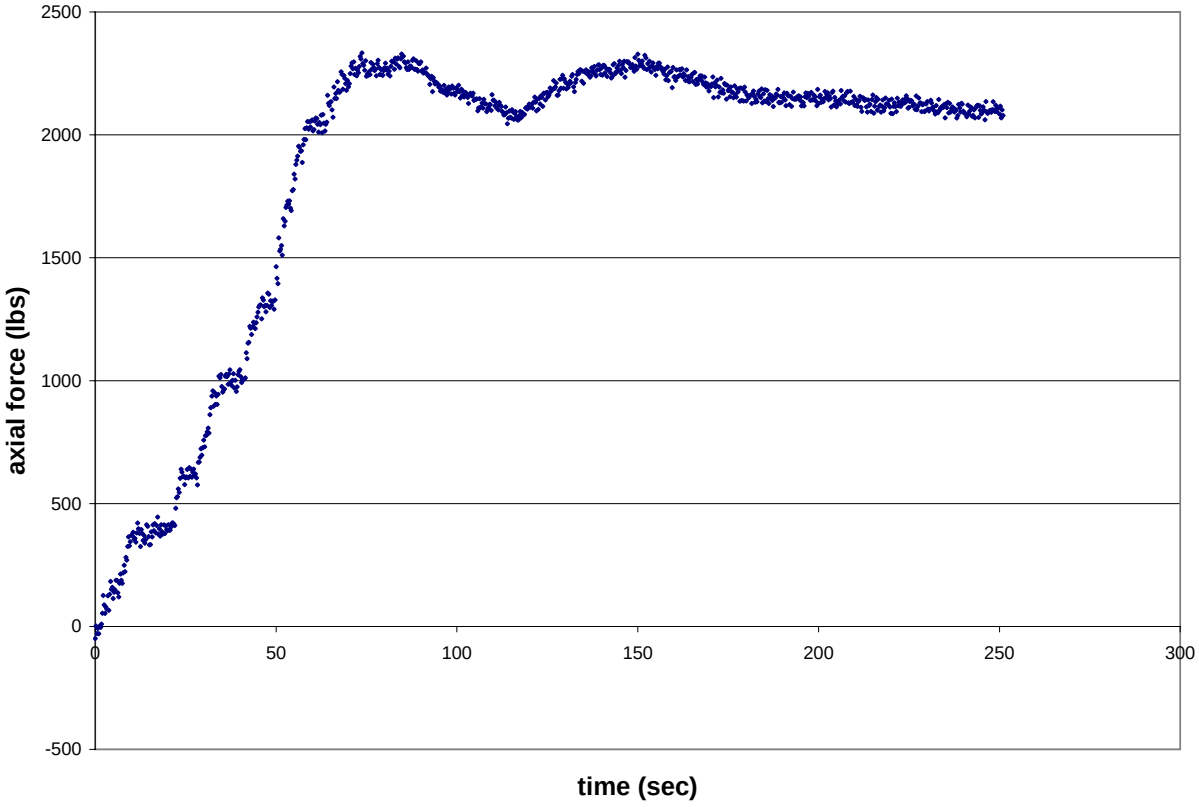

Figure 14. Force in tightened rod

The Harshman Bridge was next tested by traversing the span with a 12-ton truck provided by the Preble County Highway Department. Three runs were made, the first and third time stopping at the locations shown in Figure 15, and the second time driving through nonstop. Data from the tests are discussed in conjunction with the analytical predictions in the following sections.

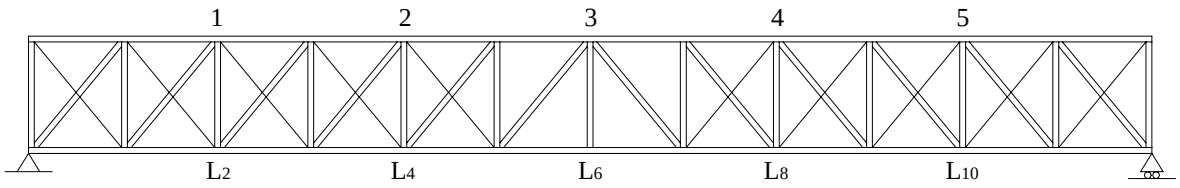

Figure 15. Truck stops (west truss) for Runs 1 and 3

Modeling and Analyses of the Harshman Bridge

A necessary first step was to calculate the dead weight of the bridge and to compute geometric properties of the cross-sections. The floor was assumed to be oak with a unit weight of 44 lbs/ft^3. All other wood components were assumed to be yellow pine, with a unit weight of 38 lb/ft^3. Table 1 lists contributions of the trusses, siding, deck, and roof to the total weight, which was estimated to be 95,400 lbs. This figure was increased by 10 percent to account for uncertainties and miscellaneous connection parts. Therefore a total dead weight of 104,900 lbs was used for analysis.

It was assumed that all wood members have the same modulus of elasticity, E, equal to 1,200,000 lbs/in^2. The modulus of the iron was assumed to be 28,000,000 lbs/in^2. Table 2 summarizes element areas, moments of inertia, section moduli, and axial stiffnesses, EA/L. The axial stiffnesses of the compression wood diagonals are approximately three times the axial stiffnesses of the corresponding tension iron diagonals.

Table 1. Total weight of the Harshman Bridge

Member	Height	Length/diameter	Depth	Volume	Quantity	Density	Weight
	(ft)	(ft)	(ft)	(cu.ft.)		(lbs/cu.ft.)	(lbs)
Truss							
Top chords	0.656	97.860	1.333	85.628	1	38.000	3253.8
Bottom chords	1.000	97.860	1.333	130.480	1	38.000	4958.2
Verticals	13.760	0.573	0.573	4.517	13	38.000	2231.2
Compressive diagonals U_0L_0, $U_{11}L_{12}$	13.219	0.646	1.000	8.537	2	38.000	648.9
U_2L_1, $U_{10}L_{11}$	13.219	0.563	1.000	7.436	2	38.000	565.1
U_3L_2, U_9L_{10}	13.219	0.479	1.000	6.334	2	38.000	481.4
U_8L_9	13.219	0.417	1.000	5.508	1	38.000	209.3
U_4L_3	13.219	0.396	1.000	5.233	1	38.000	198.8
U_7L_8	13.219	0.333	1.000	4.406	1	38.000	167.4
U_5L_4	13.219	0.313	1.000	4.131	1	38.000	156.9
U_6L_7	13.219	0.250	1.000	3.305	1	38.000	125.6
U_6L_5	13.219	0.229	1.000	3.029	1	38.000	115.1
Tension rods U_0L_1, U_1L_2, $U_{11}L_{10}$, $U_{12}L_{11}$	16.897	0.104	-	0.144	4	484.000	278.8
U_2L_3, U_3L_4, U_9L_8, $U_{10}L_9$	16.897	0.094	-	0.117	4	484.000	225.8
U_4L_5, U_8L_7	16.897	0.083	-	0.092	2	484.000	89.2
Total weight of trusses (x2)							**27410**
Siding							
Panels	13.188	97.860	0.083	107.544	1	38.000	4086.7
Purlins	0.333	97.860	0.167	5.437	4	38.000	826.4
Railing	1.000	97.860	0.083	8.155	1	38.000	309.9
Total siding weight (x2)							**10450**
Deck							
Girders	15.958	0.500	1.125	8.977	24	44.000	9479.3
Joists	8.000	0.250	0.500	1.000	174	44.000	7656.0
Cross-bracing	7.614	0.333	0.417	1.058	48	44.000	2233.4
Deck (transverse)	15.958	97.860	0.250	390.421	1	44.000	17178.5
Deck (wear surface)	15.958	97.860	0.167	260.280	1	44.000	11452.3
Total deck weight							**48000**
Roof							
Bracing	4.214	0.333	0.333	0.468	26	38.000	462.6
Beams	15.958	0.500	0.500	3.990	13	38.000	1970.9
Cross-bracing	10.466	0.083	0.583	0.509	48	38.000	928.0
Cross-bracing (ends)	14.880	0.083	0.583	0.723	4	38.000	109.9
Purlins	98.396	0.292	0.063	1.794	2	38.000	136.3
Rafters	9.214	0.167	0.333	0.512	50	38.000	972.6
Lathing	97.860	0.083	0.333	2.718	21	38.000	2169.2
Wood shingles	97.860	9.483	-	928.006	1	2.000	1856.0
Galvanized steel	97.860	9.483	-	928.006	1	1.000	928.0
Total roof weight							**9530**
Total bridge weight							**95390**

Table 2. Member properties

Element	Length	Area (A)	Moment of inertia (I)	Section modulus (S)	Elastic modulus (E)	Axial stiffness (k=EA/L)
	(in)	(in^2)	(in^4)	(in^3)	(psi)	(lbs/in)
Top chord	97.86	126.0	651	165.33	1,200,000	1545100
Bottom chord	97.86	192.0	2304	384.00	1,200,000	2354400
Verticals	146.22	47.27	186.2	54.17	1,200,000	382500
Compressive diagonals U_0L_0, $U_{11}L_{12}$	159.75	93.0	465.5	120.13	1,200,000	628200
U_2L_1, $U_{10}L_{11}$	159.75	81.0	307.5	91.11	1,200,000	547100
U_3L_2, U_9L_{10}	159.75	69.0	190.1	66.12	1,200,000	466100
U_8L_9	159.75	60.0	125.0	50.00	1,200,000	405300
U_4L_3	159.75	57.0	107.2	45.14	1,200,000	385000
U_7L_8	159.75	48.0	64.00	32.00	1,200,000	324200
U_5L_4	159.75	45.0	52.73	28.12	1,200,000	304000
U_6L_7	159.75	36.0	27.00	18.00	1,200,000	243200
U_6L_5	159.75	33.0	20.80	15.13	1,200,000	222900
Tension rods U_0L_1, U_1L_2, $U_{11}L_{10}$, $U_{12}L_{11}$	202.77	1.227	0.120	0.192	28,000,000	193400
U_2L_3, U_3L_4, U_9L_8, $U_{10}L_9$	202.77	0.994	0.0786	0.140	28,000,000	156700
U_4L_5, U_8L_7	202.77	0.785	0.0491	0.0982	28,000,000	123700

Two mathematical models of the Harshman Bridge were defined. One was a plane truss model that was used for approximate manual analyses. The other was a plane frame model for computer structural analyses. The plane truss model is shown in Figure 16. The model assumes symmetry about the midspan, therefore it was used only for symmetric dead and live loads. The model is statically indeterminate to the fifth degree. Sherman almost certainly used some approximate manual analysis procedure to estimate member forces. Here it was assumed that the vertical component of the force in a diagonal was equal to the total shear in the panel times the ratio of the axial stiffness of the diagonal to the sum of the axial stiffnesses of the two diagonals.

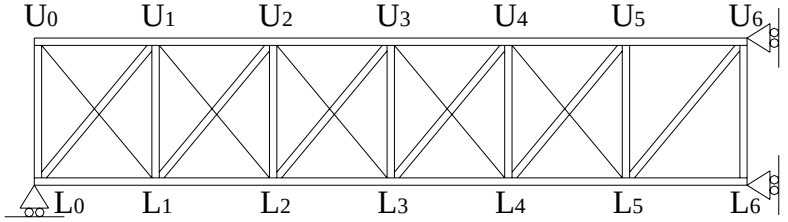

Figure 16. Plane truss model used for manual analyses

The plane frame model is shown in Figure 17. Moment connections were assumed for all members. It was assumed that all girders were supported at the quarter points of the panels, therefore nodes were defined at those points.

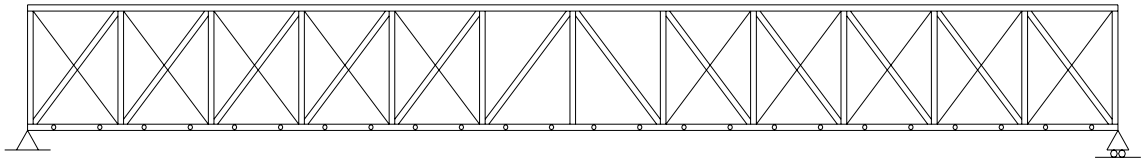

Figure 17. Plane frame model used for computer analyses

Dead Load Analyses and Behavior

To compute effects of self-weight, uniformly distributed vertical loads were applied to each model. For the plane frame model, the floor dead loads were applied at the quarter-points, where the girders are supported. Table 3 compares member axial forces computed using the approximate manual analysis with corresponding forces calculated by computer analysis (using MASTAN2).

Table 3. Results of dead load analyses

Member	Manually calculated force	MASTAN2 calculated force	Difference
	(kips)	(kips)	(kips)
Top chord			
U_0U_1	-3.291	-3.794	0.503
U_1U_2	-18.957	-21.179	2.222
U_2U_3	-31.257	-32.493	1.236
U_3U_4	-41.021	-41.843	0.822
U_4U_5	-47.533	-47.984	0.451
U_5U_6	-50.772	-50.879	0.107
Bottom chord			
L_0L_1	12.666	12.3	0.366
L_1L_2	26.013	24	2.013
L_2L_3	36.923	35.868	1.055
L_3L_4	44.566	43.889	0.677
L_4L_5	49.659	49.373	0.286
L_5L_6	52.223	52.183	0.04
Verticals			
U_0L_0	-6.291	-7.005	0.714
U_1L_1	13.36	9.239	4.121
U_2L_2	10.548	5.645	4.903
U_3L_3	7.885	4.918	2.967
U_4L_4	5.2	3.492	1.708
U_5L_5	3.612	2.991	0.621
U_6L_6	1.55	2.775	1.225
Compression diagonals			
U_1L_0	-23.009	-22.093	0.916
U_2L_1	-18.268	-14.284	3.984
U_3L_2	-14.37	-12.165	2.205
U_4L_3	-9.808	-8.385	1.423
U_5L_4	-5.884	-5.196	0.688
U_6L_5	-2.635	-2.368	0.267
Tension rods			
U_0L_1	5.978	6.785	0.807
U_1L_2	5.449	9.245	3.796
U_2L_3	4.076	6.077	2.001
U_3L_4	3.368	4.691	1.323
U_4L_5	2.022	2.682	0.66

There was excellent agreement in chord forces and very good agreement in the diagonal forces. The forces in the verticals predicted by the two models show greater percent differences. In general, the close agreement between forces computed using the two

models indicates that the bridge acts primarily as a truss and that approximate manual analyses may be adequate for design.

Results of the computer analysis show the tension rods carry a greater percentage of the shear force in each panel than assumed in the manual analysis. Table 4 shows the ratio of the computer-calculated forces versus that used in the manual calculations. The closest correspondence between the ratios can be seen in the first ($U_0U_1L_1L_0$) panel of the truss, where the outermost diagonal sees a large force from the support.

Table 4. Stiffness and force ratios for diagonal members

Compression diagonal	Tension rod	Ratio of K values = Assumed ratio of manually calculated forces	Ratio of MASTAN2 calculated forces
U_1L_0	U_0L_1	3.85	3.26
U_2L_1	U_1L_2	3.35	1.55
U_3L_2	U_2L_3	3.52	2.00
U_4L_3	U_3L_4	2.91	1.79
U_5L_4	U_4L_5	2.91	1.94

As seen in Table 3, dead load forces in the diagonal members decrease towards the midspan of the truss, which forms the basis for Sherman's decision to decrease the size of the diagonal members. Tables 5 and 6 show dead load axial stresses in the diagonals. The magnitudes are comparable along the span, which attests to the rationality of Sherman's decrease in the member sizes towards the midspan.

Table 5. Axial stresses in the compression diagonals

Compression diagonal	Cross-section area	Manually calculated force	Axial stress	MASTAN2 calculated force	Axial stress
	(sq. in.)	(kips)	(ksi)	(kips)	(ksi)
U_1L_0	93.0	-23.009	0.247	-22.093	0.238
U_2L_1	81.0	-18.268	0.226	-14.284	0.176
U_3L_2	69.0	-14.370	0.208	-12.165	0.176
U_4L_3	57.0	-9.808	0.172	-8.385	0.147
U_5L_4	45.0	-5.884	0.131	-5.196	0.115
U_6L_5	33.0	-2.635	0.080	-2.368	0.072

Table 6. Axial stresses in the tension rods

Tension Rod	Cross-section area	Manually calculated force	Axial stress	MASTAN2 calculated force	Axial stress
	(sq. in.)	(kips)	(ksi)	(kips)	(ksi)
U_0L_1	1.227	5.978	4.872	6.785	5.530
U_1L_2	1.227	5.449	4.441	9.245	7.535
U_2L_3	0.994	4.076	4.101	6.077	6.114
U_3L_4	0.994	3.368	3.388	4.691	4.719
U_4L_5	0.785	2.022	2.576	2.682	3.417

For the plane frame model, the members have both axial forces and bending moments. Table 7 shows stresses from axial forces and maximum combined stresses from both axial forces and bending moments in four members. Bending moments contribute 10 to 40 percent to the combined maximum stresses. The maximum combined dead load stresses are greater in the compressive top chord than in the tensile bottom chord. The maximum combined dead load stresses are less than 500 lbs/in^2 in all cases.

The vertical dead load displacement at midspan for the truss model was also calculated manually (using the Principle of Virtual Forces). It was estimated to be 0.834". The midspan vertical displacement for the plane frame model was predicted to be 0.773". It was expected that the plane frame model should have smaller displacements because of the addition of the flexural stiffness of the members. For both models, the predicted displacements depend on the assumption of the modulus of elasticity, which is highly uncertain.

Table 7. Effect of combined stresses

Element	Cross-section area	Section modulus	MASTAN2 calculated force	MASTAN2 calculated moment	Axial stress	Combined stress	% Contribution from moment
	(sq. in.)	(cu. In.)	(kips)	(k-in)	(ksi)	(ksi)	
Vertical U_0L_0	47.27	54.17	-7.005	5.259	0.148	0.245	39.6
Compression diagonal U_1L_0	93	120.13	-22.093	9.667	0.238	0.318	25.3
Top chord U_5U_6	126.0	165.3	-50.879	7.615	0.404	0.450	10.2
Bottom chord L_5L_6	192.0	384.0	52.183	27.748	0.272	0.344	21.0

Live Load Analyses and Behavior

Four live load conditions were considered. The first was a unit vertical load at midspan, in order to compare predictions of the two models. The second was a moving vertical load in order to determine influence lines that may be compared with the data from the tests. The other two were uniformly distributed live loads of 80 lbs/ft^2 over the entire

span and over half the span. These latter live load conditions were studied to estimate the maximum stresses in the members for a typical nineteenth century distributed live load. Table 8 shows element axial forces for a unit vertical live load at midspan in the two models. As for the dead loads, the chord forces from the two models are in good agreement, whereas the forces in the vertical members have greater percentage differences.

Table 8. Results of live load analysis, 1 kip load at center of truss (negative value indicates compression)

Element	Manually calculated force	MASTAN2 calculated force	Difference
	(kips)	(kips)	(kips)
Top chord			
U_0U_1	-0.068	-0.080	0.0122
U_1U_2	-0.406	-0.453	0.047
U_2U_3	-0.733	-0.767	0.034
U_3U_4	-1.074	-1.102	0.028
U_4U_5	-1.404	-1.441	0.037
U_5U_6	-1.650	-1.668	0.018
Bottom chord			
L_0L_1	0.262	0.249	0.013
L_1L_2	0.583	0.536	0.047
L_2L_3	0.915	0.881	0.034
L_3L_4	1.234	1.203	0.031
L_4L_5	1.564	1.539	0.025
L_5L_6	1.978	1.934	0.044
Verticals			
U_0L_0	-0.068	-0.121	0.053
U_1L_1	0.282	0.184	0.098
U_2L_2	0.274	0.149	0.125
U_3L_3	0.261	0.161	0.1
U_4L_4	0.244	0.138	0.106
U_5L_5	0.374	0.316	0.058
U_6L_6	0.500	0.840	0.34
Compression diagonals			
U_1L_0	-0.476	-0.449	0.027
U_2L_1	-0.461	-0.372	0.089
U_3L_2	-0.466	-0.400	0.066
U_4L_3	-0.446	-0.386	0.06
U_5L_4	-0.446	-0.404	0.042
U_6L_5	-0.599	-0.481	0.118
Tension rods			
U_0L_1	0.123	0.144	0.021
U_1L_2	0.138	0.224	0.086
U_2L_3	0.133	0.194	0.061
U_3L_4	0.153	0.204	0.051

U_4L_5	0.153	0.226	0.073

Table 9 shows the assumed and computed (using MASTAN2) ratios of the axial forces in the compressive diagonals to the axial forces in the tension rods. The assumption that the shear in each panel was shared by the diagonal members in proportion to their axial stiffnesses over-estimates the force taken by the compression diagonals.

Table 9. Load sharing in diagonal members from a 1 kip vertical load at midspan

Compression diagonal	Tension rod	Ratio of K values = Assumed ratio of manually calculated forces	Ratio of MASTAN2 calculated forces
U_1L_0	U_0L_1	3.85	3.12
U_2L_1	U_1L_2	3.35	1.66
U_3L_2	U_2L_3	3.52	2.06
U_4L_3	U_3L_4	2.91	1.89
U_5L_4	U_4L_5	2.91	1.79

Tables 10 and 11 show stresses from axial forces produced by the 1 kip vertical load at midspan. In order to assess the relative importance of live loads and dead loads, these stresses should be multiplied by a reasonable design concentrated live load, such as the current load limit of 12 kips (or 12 tons on the entire bridge).

Table 10. Axial stress in compression diagonals from a 1 kip vertical load at midspan

Compression diagonal	Cross-section area	Manually calculated force	Axial stress	MASTAN2 calculated force	Axial stress
	(sq. in.)	(kips)	(ksi)	(kips)	(ksi)
U_1L_0	93.0	-0.476	0.00512	-0.449	0.00483
U_2L_1	81.0	-0.461	0.00569	-0.372	0.00459
U_3L_2	69.0	-0.466	0.00675	-0.400	0.00580
U_4L_3	57.0	-0.446	0.00782	-0.386	0.00677
U_5L_4	45.0	-0.446	0.00991	-0.404	0.00898
U_6L_5	33.0	-0.599	0.01815	-0.481	0.01458

Table 11. Axial stress in tension rods from a 1 kip vertical load at midspan

Tension Rod	Cross-section area	Manually calculated force	Axial stress	MASTAN2 calculated force	Axial stress
	(sq. in.)	(kips)	(ksi)	(kips)	(ksi)
U_0L_1	1.227	0.123	0.100	0.144	0.117
U_1L_2	1.227	0.138	0.112	0.224	0.183
U_2L_3	0.994	0.133	0.134	0.194	0.195
U_3L_4	0.994	0.153	0.154	0.204	0.205
U_4L_5	0.785	0.153	0.195	0.226	0.288

The effects of moments from the one kip live load on maximum stresses are given in Table 12. The four members see between a 20 to 60 percent increase in stress with the addition of the moments.

Table 12. Combined stress under the 1 kip at center live load condition

Element	Cross-section area	Section modulus	MASTAN2 calculated force	MASTAN2 calculated moment	Axial stress	Combined stress	% Contribution from moment
	(sq. in.)	(cu. In.)	(kips)	(k-in)	(ksi)	(ksi)	
Vertical U_0L_0	47.27	54.17	-0.121	0.0837	0.0026	0.0041	37.6
Compression diagonal U_1L_0	93	120.13	-0.449	0.150	0.0048	0.0061	20.5
Top chord U_5U_6	126.0	165.3	-1.668	1.214	0.0132	0.0206	35.7
Bottom chord L_5L_6	192.0	384.0	1.934	5.632	0.0101	0.0247	59.3

The midspan vertical displacement from the one kip load at midspan was found to be 0.0308” by the manual calculations and 0.0287” by the computer analysis. As before, the smaller value predicted by the MASTAN2 analysis results from consideration of the axial and flexural stiffness by the program as opposed to only considering the axial stiffness in the manual calculations.

Using the results of computer analyses for the 1 kip load traversing the bottom chord, influence lines were plotted for vertical displacements at two nodes and for axial forces in key members of the bridge. Figure 18 shows vertical displacements at two nodes as a function of position of the unit load.

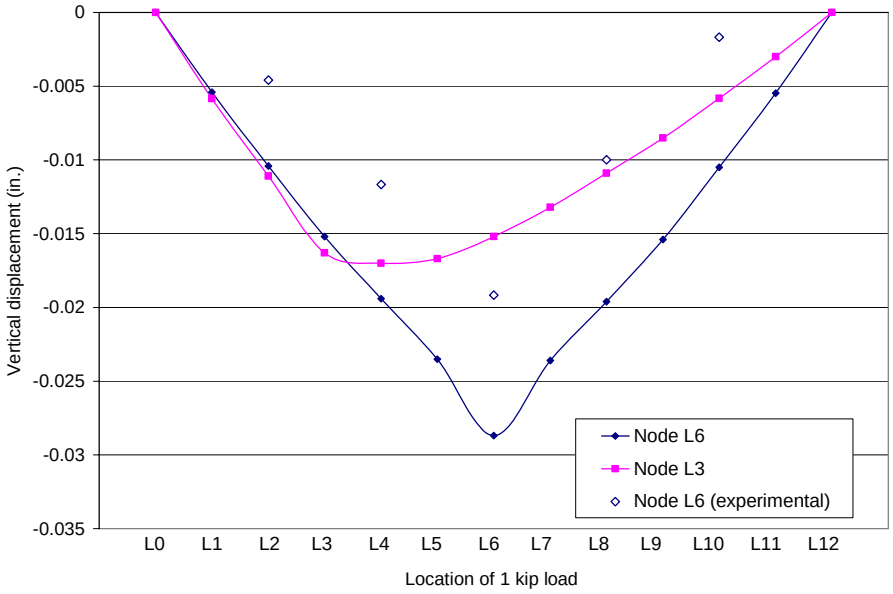

Figure 18. Influence lines for the vertical displacements of two nodes

Figures 19 through 23 show analytical influence lines for axial forces in nine truss members.

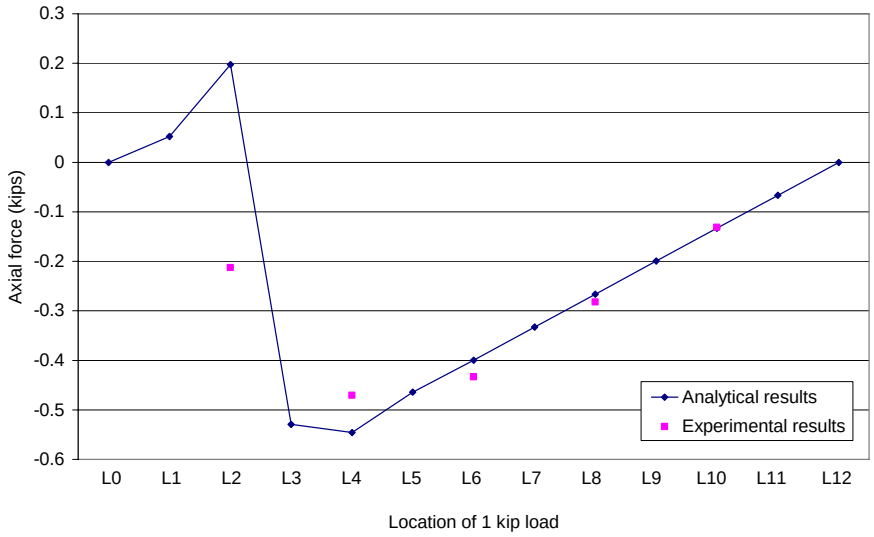

Figure 19. Influence line for compression diagonal U_3L_2

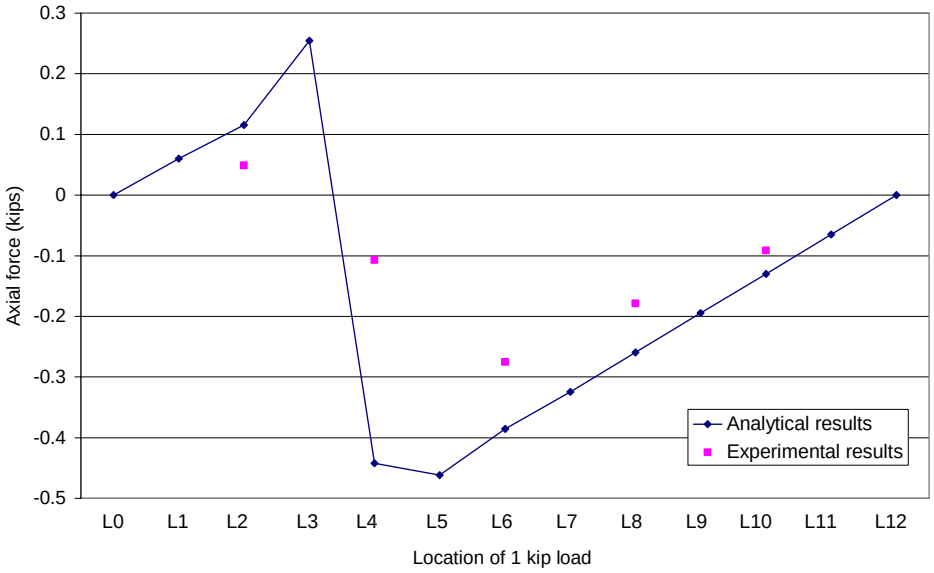

Figure 20. Influence line for compression diagonal U_4L_3

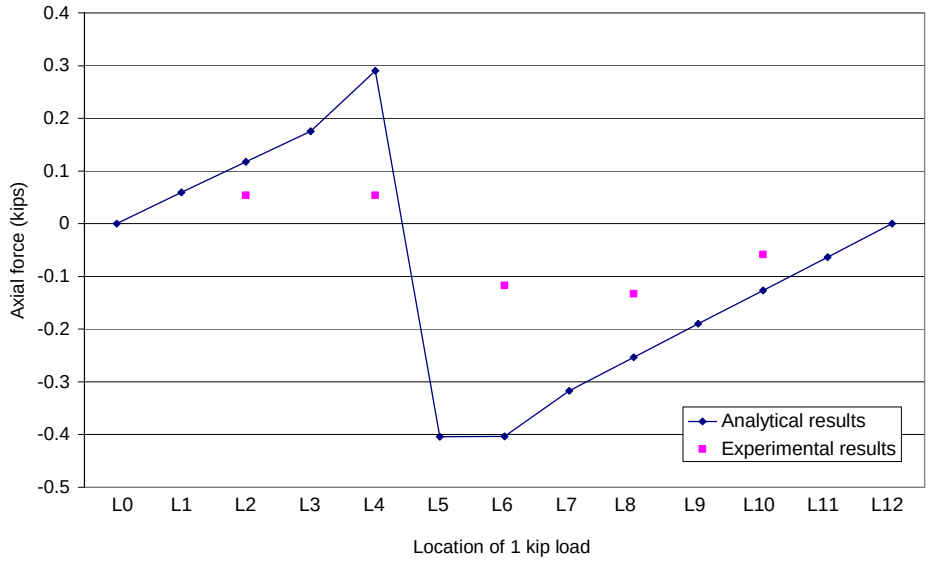

Figure 21. Influence line for compression diagonal U_5L_4

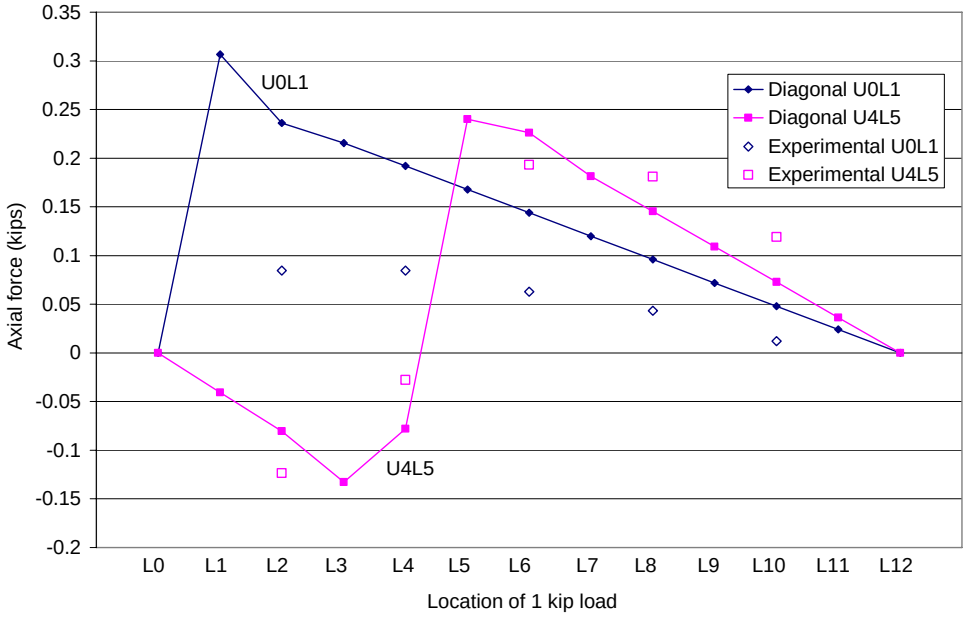

Figure 22. Influence lines for tension rods U_0L_1 and U_4L_5

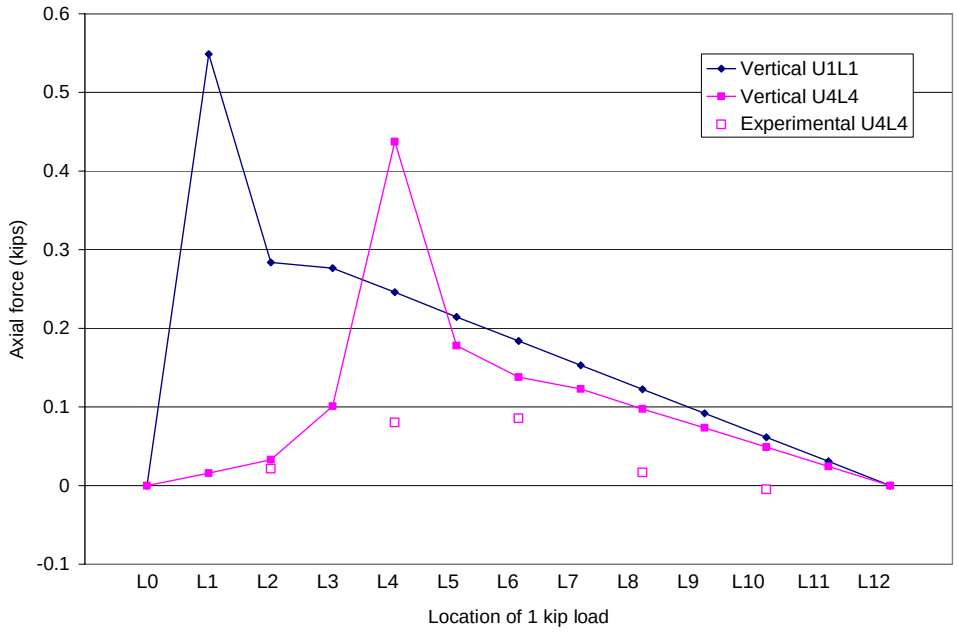

Figure 23. Influence lines for axial forces in vertical elements U_1L_1 and U_4L_4

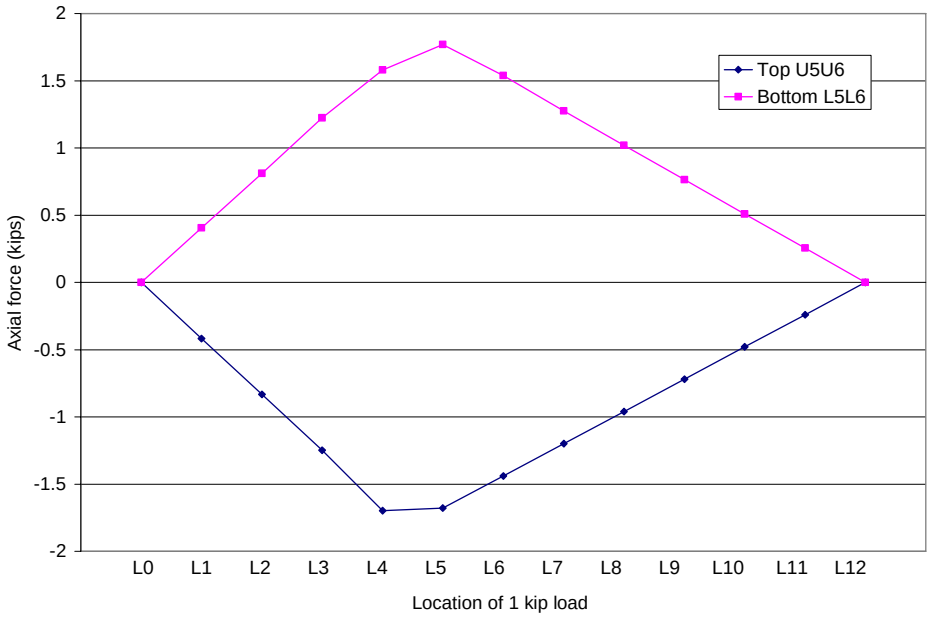

Figure 24. Influence lines for top chord U5U6 and bottom chord L5L6

Figures 25, 26, and 27 show time histories of member axial forces and vertical displacements obtained from the physical load tests. "Plateaus" in the data correspond to periods during which the truck was stopped with its center of gravity at the nodes. The fluctuations at the ends of each plateau result from the truck decelerating/accelerating.

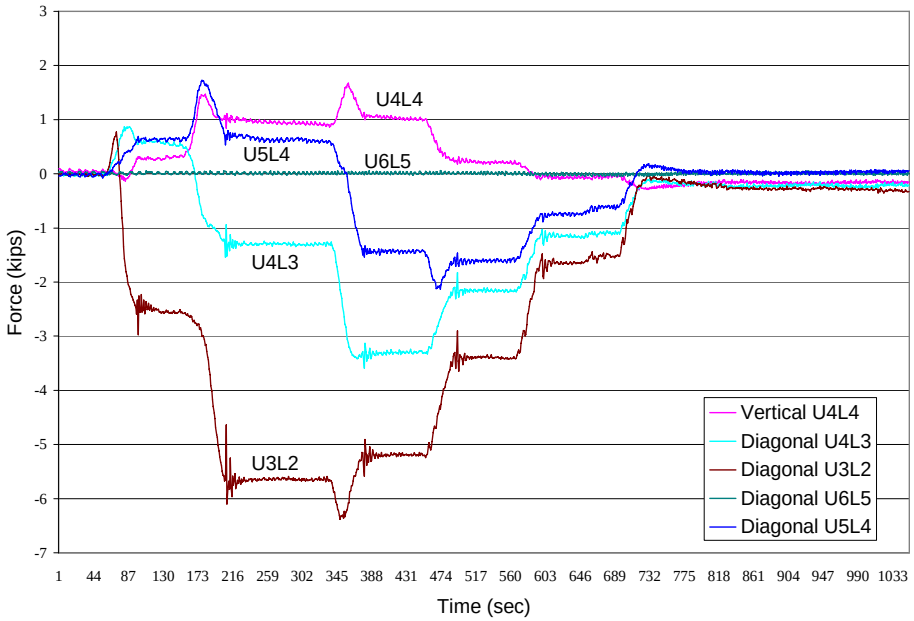

Figure 25. Axial force in wood elements instrumented with strain transducers, Run 1 of Test 2

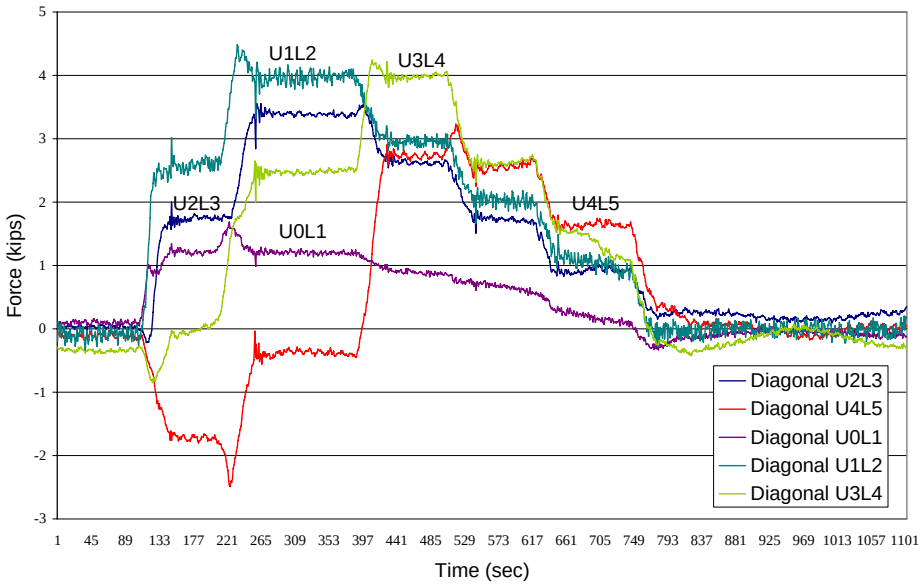

Figure 26. Axial force in iron tension rods, Run 1 of Test 2

Figure 25 shows that the force in diagonal U_6L_5 was practically zero for all positions of the truck. Assuming that the transducer was functioning properly, this would indicate that the diagonal was effectively loose. Diagonal U_5L_4 shows the greatest reversal of force from the live load, which shows the need for a compressive force from dead load to prevent looseness. The maximum compressive force from the moving load occurs in diagonal U_3L_2. The vertical member, U_4L_4, remains in tension for all positions of the moving load.

Figure 26 shows that tension rod U_4L_5 had the greatest force reversal from the live load, which shows the need for a tensile force from the dead load to prevent buckling. Diagonal U_0L_1 had a tensile force for all positions of the load.

Figure 27 shows the experimental vertical displacements at the midspan of the east and west trusses. The displacements of the two trusses should not be the same for any one position of the load because of the skewness of the bridge. The displacements of the west truss would be symmetric if the truss was truly symmetric, which is not possible due to variations in the member sizes and in the mechanical properties of wood.

The experimental load effects in Figures 25, 26, and 27 are for a 12-ton truck traversing the span. If it is assumed that each truss carried half the truck weight, then the experimental responses at the “plateaus” may be divided by 12 and compared with the analytical influence lines. These experimental responses are plotted together with the analytical influence lines in Figures 18 to 23.

Experimental and analytical influence lines for midspan vertical displacement (Figure 18) and for axial forces in members U_3L_2 (Figure 23) and U_4L_5 (Figure 22) are in very good agreement. Experimental and analytical influence lines for axial forces in the other members that were instrumented show greater differences, although variations with position are similar. Tables 13 and 14 compare analytical and experimental axial stresses in the instrumented members for the five locations at which the truck was stopped. Although the plane frame model captured the overall bridge behavior in terms of midspan vertical displacement, the analytical and experimental results for member axial forces and stresses were not in uniform agreement for all members.

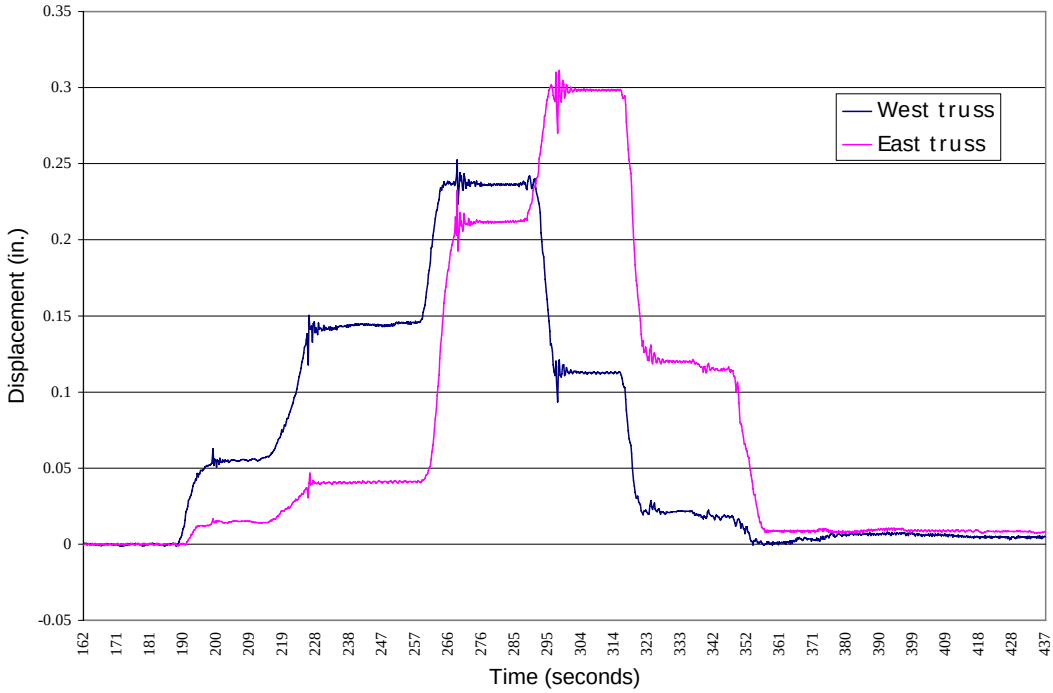

Figure 27. Midspan vertical displacement under 12-ton truck, Run 1 of Test 2

Table 13. Experimental axial stress in elements during Run 1 of Test 2 (negative value indicates compression)

	Location of 1 kip load				
Element	**L2**	**L4**	**L6**	**L8**	**L10**
Vertical U_4L_4	0.00546	0.0204	0.0217	0.00420	-0.00129
Compression diagonal U_3L_2	-0.0370	-0.0818	-0.0753	-0.0491	-0.0228
Compression diagonal U_4L_3	0.0103	-0.0225	-0.0579	-0.0377	-0.0192
Compression diagonal U_5L_4	0.0144	0.0144	-0.0312	-0.0354	-0.0156
Compression diagonal U_6L_5	0	0	0	0	0
Tension rod U_0L_1	0.827	0.827	0.614	0.425	0.118
Tension rod U_1L_2	1.654	2.718	2.032	1.394	0.685
Tension rod U_2L_3	1.489	2.859	2.245	1.465	0.827
Tension rod U_3L_4	0	2.103	3.382	2.245	1.134
Tension rod U_4L_5	-1.891	-0.425	2.954	2.765	1.820

Table 14. Live load axial stress in elements by computer analysis (negative value indicates compression)

	Location of 1 kip load				
Element	**L2**	**L4**	**L6**	**L8**	**L10**
Vertical U_4L_4	-0.00831	0.111	0.0351	0.0247	0.0124
Compression diagonal U_3L_2	0.0344	-0.0949	-0.0695	-0.0463	-0.0231
Compression diagonal U_4L_3	0.0243	-0.0931	-0.0812	-0.0547	-0.0273
Compression diagonal U_5L_4	0.0314	0.0774	-0.108	-0.0676	-0.0338
Compression diagonal U_6L_5	0.0701	0.142	-0.175	-0.141	-0.0707
Tension rod U_0L_1	2.310	1.880	1.407	0.938	0.469
Tension rod U_1L_2	4.017	2.912	2.188	1.460	0.730
Tension rod U_2L_3	0.305	3.094	2.344	1.556	0.778
Tension rod U_3L_4	-1.085	3.763	2.464	1.666	0.833
Tension rod U_4L_5	-1.232	-1.191	3.458	2.224	1.112

Uniform Live Load Analyses

To help assess Sherman's design, it is meaningful to estimate maximum normal stresses in the members under a combination of dead load and a common nineteenth century uniformly distributed design live load. At the end of the nineteenth century, Ketchum proposed an 80 lbs/ft^2 live load for spans under 75 ft, 55 lbs/ft^2 for spans reaching 200 ft, and a linear variation in load for spans between 75 and 200 ft[17]. A conservative live load of 80 lbs/ft^2 was assumed for the Harshman Bridge.

The two uniform live load cases modeled for the Harshman Bridge were a uniform live load of 80 lbs/ft^2 over the entire span of the bridge, and a uniform live load of 80 lbs/ft^2 over half the span of the bridge. Both live load cases were analyzed with the dead load on the bridge as well. Maximum normal stresses from axial forces and bending moments for a set of members are given in Table 15.

[17] M.S. Ketchum, *The Design of Highway Bridges and the Calculation of Stresses in Bridge Trusses* (New York: The Engineering News Publishing Company, 1909).

Table 15. Results of uniform live load analyses

Element	Stress due to 80 psf over half-span	Stress due to 80 psf over full span
	(ksi)	(ksi)
Top chord U_5U_6	-0.646	-0.812
Top chord U_6U_7	-0.505	-0.812
Bottom chord L_5L_6	0.760	1.030
Bottom chord L_6L_7	0.717	1.030
Vertical U_1L_1	0.400	0.465
Vertical U_6L_6	0.114	0.166
Vertical $U_{11}L_{11}$	0.261	0.465
Compression diagonal U_2L_1	-0.317	-0.394
Compression diagonal U_6L_5	0.139	-0.160
Compression diagonal U_6L_7	-0.343	-0.150
Compression diagonal $U_{10}L_{11}$	-0.254	-0.394
Tension rod U_0L_1	11.12	13.09
Tension rod U_4L_5	3.60	8.26
Tension rod U_8L_7	7.91	8.10
Tension rod $U_{12}L_{11}$	7.50	13.09

Allowable normal stresses in pine range between 850 psi and 1750 psi, and most of the elements fell well below the minimum value of this range. The exception to this was the bottom chord of the truss, which fell in the lower part of this allowable range. The allowable axial stress in wrought iron ranges between 13000 and 15000 psi, and maximum stresses in the tension rods were within this range.

Live load vertical displacements at midspan for the two uniform live load conditions were 0.5” for the load over half-span and 1.0” for the load over the full span. That is, the maximum live load displacement was approximately 1/1200 of the span, which means that the bridge has a high, acceptable live load stiffness.

Table 15 shows that the model predicted a *tensile* force in diagonal U_6L_5 for an 80 lbs/ft^2 live load over half the span. This was not possible given the simple bearing connections used for the wood diagonals, which meant the model was inappropriate for an 80 lbs/ft^2 live load over half the span. By setting the total dead load and live load axial force in member U_6L_5 equal to zero, the magnitude of the uniformly distributed live load over half the span that caused this condition could be inferred. For the plane frame model used, it was estimated that that a load of 57 lbs/ft^2 over half the span would cause member U_6L_5 to become loose. Similarly, a concentrated vertical load of 9.5 kips at node L_5 would cause compression diagonal U_6L_5 to become loose. This value was significantly lower than the 12 kips used in the experiment, which may explain the zero force in the compression diagonal in the results (Figure 25).

Of course the capacity of a bridge also depends on the capacity of its floor system. Sherman used closely-spaced girders supported by wrought iron hangers. With such supports, the girders may be modeled as simply supported beams. With such a model, the maximum flexural normal and shear stresses for dead load plus an 80 lbs/ft^2 live load are 1083 lbs/in^2 and 72.2 lbs/in^2, respectively. These are below the typical allowable stresses for red oak, which are 1100 lbs/in^2 and 155 lbs/in^2, respectively. The steel beams (W12x35 sections) were recently added to help carry the loads. These steel beams decrease the maximum flexural normal stresses in the wood beams, but because of the connection detail used, they increase the maximum shear stress in the wood girders (which have to support the weight of the steel beams). The wood girders and the steel beams share in carrying live loads in proportion to their flexural stiffnesses. For example, the fraction of the total load carried by the wood girders is equal to the ratio:

$$\frac{\mathbf{E_w I_w}}{\mathbf{E_w I_w + E_s I_s}}$$

in which E_w and E_s are the modulus of elasticity of the wood and steel sections and I_w and I_s are the moments of inertia of the wood and steel sections. Substituting the actual values of these parameters shows that the steel beam reduces the maximum normal stress in the wood girder by 85 percent. Conversely, the maximum shear stress in the wood girder increases by approximately 8 percent.

Construction and Tightening the Nuts on the Rods

The construction process for the Harshman Bridge, as well as most covered bridges, is unknown, particularly at the time the nuts were tightened. It is very likely that falsework was built with the desired camber. The chords, verticals, and diagonal members were then placed and connected, but the framework did not support its self-weight, which was carried by the falsework. The rods were probably placed next. The nuts could not be tightened as in a Howe or Pratt truss because tightening would simply distort a panel since the connections of the wood diagonals precluded tension. Therefore it is likely that the nuts were only “snug-tightened” when the falsework was in place. As the falsework was removed, the dead load was transferred to the truss. The two analytical models presented here estimate the dead load member forces for such a construction scenario.

Once the self-weight was transferred to the truss, further tightening of the nuts would change the dead load forces in the members. It is not certain whether this could have been achieved with manual tightening methods. Moreover, there do not seem to be clear advantages for doing so for a Childs-type truss, since the tensile iron diagonals and the compressive wood diagonals were already able to contribute to carrying the live load.

Nonetheless, to estimate the effects of tightening a nut with the falsework removed and the compressive wood diagonals active, analyses of the plane frame models were performed for effective unit loads from tightening nuts. Figure 28a shows member axial

forces and vertical displacements of L_1 and L_2 from unit effective forces from tightening rods U_1L_2 and $U_{11}L_{10}$ at the same time. Figure 28b shows member axial forces and vertical displacements of nodes L_4 and L_5 from unit effective forces from tightening rods U_4L_5 and U_8L_7 at the same time. The figures show that tightening the rods increased dead load tensile forces in the rods, decreased the dead load compressive forces in the wood diagonals and decreased the dead load tensile forces in the verticals. Member axial forces in adjacent panels were an order of magnitude smaller than those in the panel where the rods were tightened. The tightening action caused very small upward vertical displacements of the nodes, therefore tightening was not an effective method to induce camber in the truss.

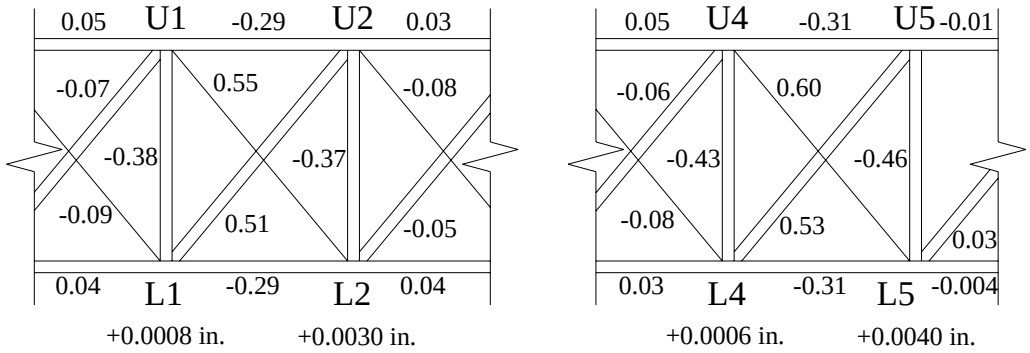

(a) **(b)**

Figure 28. Forces (in kips) and displacements (in inches) in truss elements resulting from tightening of U_1L_2 (left) and U_4L_5 (right)

Time-Dependent Behavior of the Harshman Bridge

Wood has time-dependent stress-strain behavior at ambient temperatures, thus it is can be considered to be a viscous material. For example, if a constant stress is applied to wood, the strain increases with time. This phenomenon is called creep, and it occurs in three stages; the first stage of creep deformation occurs when the structure is first loaded, the second stage is reached when the rate of creep begins to approach zero, and third stage, which occurs under large loads over long periods of time, is when the rate of creep increases quickly to failure. The second stage is typically reached within a short period of time, and it can last for many years.[18]

[18] Forest Products Laboratory, *Wood Handbook, Wood as an Engineering Material* (Madison, WI: USDA Forest Service, 1999).

Viscous stress-strain (constitutive) models are needed in order to obtain time histories of the responses such as nodal displacements and element forces. These viscous constitutive models lead to ordinary differential equations for the effects of any loading. In lieu of such models, to obtain a qualitative sense of the effects of creep, it was assumed that all the wood elements have a creep strain, ε_{creep}, equal to ±0.0005, and that all the iron members do not creep. These assumed wood creep strains were used to compute effective nodal loads for a computer analysis of the plane frame model. The computed changes in member forces due to creep are given in Table 16.

Table 16. Element forces due to creep (negative value indicates compression)

Element	Change in member force due to assumed creep strains
	(kips)
Top chord	
U_0U_1	-8.8
U_1U_2	-7.2
U_2U_3	-6.5
U_3U_4	-6.4
U_4U_5	-6.5
U_5U_6	-0.6
Bottom chord	
L_0L_1	-9.0
L_1L_2	-7.5
L_2L_3	-6.9
L_3L_4	-6.4
L_4L_5	-5.7
L_5L_6	-1.2
Vertical	
U_0L_0	-13.5
U_1L_1	-25.0
U_2L_2	-21.5
U_3L_3	-20.3
U_4L_4	-19.6
U_5L_5	-9.8
U_6L_6	-4.6
Compressive diagonal	
U_1L_0	16.7
U_2L_1	13.6
U_3L_2	12.4
U_4L_3	12.3
U_5L_4	10.8
U_6L_5	3.7

Tension rod	
U_0L_1	15.8
U_1L_2	13.4
U_2L_3	12.0
U_3L_4	11.9
U_4L_5	11.4

These changes in force may be compared with the dead load forces given in Table 3. Qualitatively, creep decreases the dead load compressive axial forces in the wood diagonals and increases the tensile axial forces in the iron diagonals. Thus, the behavior of the Harshman Bridge approaches that of a single diagonal Pratt truss, but with *compressive* vertical elements. Of course, the analysis with the assumed uniform creep strain of ±0.0005 is not strictly valid because it predicts changes in the axial forces in the wood diagonals that are larger than the dead load compressive axial forces. In addition, although the assumption that iron does not creep at ambient temperatures is appropriate, the rods induce compressive stresses perpendicular to the grain of the chords. Thus the axial forces in the rods may be affected by (perpendicular to the grain) creep in the chords. Nonetheless, the qualitative effects of creep predicted by the model seem realistic.

Displacements generated by the analysis were perhaps the most interesting results. For the assumed creep strain of 0.0005, the predicted downward vertical displacement at midspan was 1.8". Clearly, this shows why bridges were built with significant camber, to offset the displacement that would occur over time due to creep (and shrinkage).

In both the Pine Bluff Bridge (see HAER No. IN-103) and Eldean Bridge (see HAER No. OH-122), creep caused a loss of prestressing forces in the truss forms. Although the Harshman Bridge was not prestressed, these results could correspond to the loss of dead load tensile force in the verticals due to creep. The possibility for slackness, especially in the counter braces at the end spans, was noted for Pine Bluff Bridge and Eldean Bridge. This observation corresponds with the results of the Harshman Bridge analysis, where creep reduces the compressive forces in the compressive diagonals. For Long and Howe truss forms, the effects of creep could be offset by routine retightening of the prestressed elements of each form.

Of the three truss forms–Howe, Long, and Childs–different effects were observed as a result of shrinkage. The Eldean Bridge, lacking any iron elements, saw no significant stresses as a result of shrinkage because all elements possess the same physical properties. The Pine Bluff Bridge, on the other hand, was affected by shrinkage due to the different physical properties possessed by the iron and wood. The Harshman Bridge, with its iron tension rods, would likely see resultant changes in forces due to shrinkage.

Skewness

One final structural aspect of the Harshman Bridge that should be addressed is its skewness. As noted earlier, the two trusses of the bridge are offset from one another by one panel, and this has some effects on the behavior of the bridge. However, this behavior was not taken into account in any of the structural analyses because two-dimensional models were used. Three-dimensional models would be needed to predict the effects of skewness on the structural behavior of the bridge.

Due to its skewness, any load traversing the Harshman Bridge causes unequal deflections in the two trusses because the girders frame into different panel points of the two trusses. Frames connect the two trusses. The unequal vertical displacements at the two bases of a frame do not induce moments in the frame if the bases are assumed to be "pinned." In this case, the unequal vertical displacements will not cause significant load-carrying interaction between the east and west trusses. If the bases are assumed to be rotationally fixed, then the relative vertical base deflections will induce moments in the cross frames and affect the way the east and west trusses carry a load traversing along the centerline of the skew bridge.

One possible benefit of skewness is that a large live load will not cause the compression diagonals on both the east and west truss to become loose at the same time because of the one panel offset.

Conclusions and Observations

The Childs truss was patented at a time when prestressed truss forms were in use. The 1830 Long truss and the Howe truss (1840) forms were both prestressed so that the diagonal members were in compression. The 1839 Long truss and the Pratt truss (1844) placed the diagonals in tension when prestressed. In all of these forms, prestressing was critical to ensure that the two diagonals in each panel were both active. The Childs truss, on the other hand, did not require prestressing for both diagonals to be active under a load; for example, a live load at midspan created a compressive force in the wood diagonals and a tensile force in the iron rods. A similar live load in the other trusses caused a decrease in the precompression of the counter-diagonals of the 1830 Long and Howe and a decrease in the pre-tension of the counters in the 1839 Long and Pratt. The Childs truss may not have possessed the same ease of construction as the Howe truss, but the choice of materials to correspond with the forces induced under normal loads was a reasonable alternative to prestressed truss forms.

The Harshman Bridge, lacking the connection details of Horace Childs' patent, was more likely an adaptation of the Childs truss by Everett Sherman than an actual example of the Childs truss form. Another innovation of Sherman's seems to be the decrease in the cross-sectional areas of the diagonal elements. However, like the Childs form, Sherman

does omit the tension rods in the center panel where the compression diagonal was at the greatest risk of becoming loose.

Tightening of tension rod U_0L_1 resulted in a force of 2300 lbs. This experiment was intended to model tightening of the nuts when the wood diagonals were active in resisting dead load.

For the dead load analysis, the plane truss model and plane frame model yielded similar results, with the best agreement in the top and bottom chord stresses, less in the verticals, and least in the compression diagonals and tension rods. Maximum forces under dead load conditions were over 50 kips for both the top and bottom chord, about 10 kips for the verticals, about 23 kips for the compression diagonals, and 9.3 kips for the tension rods. The ratio of vertical components of the forces in the diagonals was assumed to be proportional to the stiffnesses of the members for the plane truss analysis, but the plane frame analysis yielded higher axial forces in the tension rods. Bending moments resulting from the plane frame analysis contribute between 10 and 40 percent to the total stress in each element. The plane truss model estimated a vertical displacement at midspan of 0.834", and the plane frame model predicted a 0.773" deflection.

The first live load case studied was a unit live load placed at midspan. As with the dead load analyses, there was good correspondence in the results of the two models, particularly in the chord forces. The forces in verticals, compression diagonals and tension rods had less agreement. Bending moments in the plane frame model contributed between 20 and 60 percent to the total element stress in the live load case, a higher percentage than in the dead load analysis. Midspan vertical displacement was 0.0308" for the plane truss model and 0.0209" for the plane frame model.

Influence lines were drawn for a number of truss elements by placing a 1 kip vertical live load at different nodes across the span of the bridge. These results were used for comparison with the results of the physical experiments. For the most part, the influence lines successfully predicted the trends in element forces, but values did not always correspond. The maximum force in a compression diagonal under the experimental loads was 6 kips in member U_3L_2, and looseness (zero force) in compression diagonal U_6L_5. For the tension rods, maximum forces of about 4 kips were reached in elements U_1L_2 and U_3L_4. Maximum midspan vertical displacement due to the 12-ton truck was 0.27", whereas live load analyses predicted midspan vertical displacements of 0.344" and 0.370" for the plane frame and plane truss models, respectively.

A uniform live load of 80 lbs/ft^2, a typical nineteenth century design live load, was placed over the half-span and the full span of the bridge for analysis. For the load over the entire span, maximum stresses were 1 ksi in the bottom chord, 0.8 ksi in the top chord, 0.5 ksi in verticals, 0.4 ksi in the compression diagonals, and 13 ksi in the tension rods. All of these values are within or below the acceptable range of values for pine, or wrought iron in the case of the tension rods. The uniform live load over half the span predicts looseness in compression diagonal U_6L_5, which corresponds with the experimental

results. Calculations were made to estimate the minimum loads needed to create looseness in compression diagonal U_6L_5. This condition could be generated by a uniform live load over half-span of 57 lbf/ft^2 or a concentrated load of 9.5 kips at node L_5. Maximum stresses in the wood girders with the steel beams were also checked, and these calculations indicated that the steel beams increase the maximum shear stress by 8 percent, but reduce the normal stress in the girders by 85 percent.

A tightening analysis was performed to predict the behavior of the Harshman Bridge for the condition of the truss carrying the dead load. Though little is known about the construction process of this bridge truss, it was assumed that the nuts of the rods were snug tightened while the dead load was not active. The analysis indicated an increase in the tensile forces of the tension rods, a decrease in the compressive forces of the compression diagonals, and a decrease in the tension of the verticals due to tightening of the rod in a panel. In adjacent panels, forces were an order of magnitude smaller. Maximum vertical displacements due to tightening in one panel were very small, on the order of 0.001" per 1 kip effective tightening force.

Creep analyses were performed assuming a ±0.0005 strain due to creep. Unlike the all-wood Long truss form, this analysis indicated that the different material properties (iron and wood) in the Harshman Bridge allow creep in the wood to cause a redistribution of forces. A comparison of the creep analysis (using the assumed creep strain) to the results of the dead load analysis (with no creep strain) indicates that the compression diagonals would be relieved of a significant amount of their compressive force, the verticals would reverse signs from tension to compression, and the tension in the rods would increase. A very large vertical displacement at midspan of 1.8" downward was predicted.

Overall, there was good correspondence between the analytical predictions of the models and the experimental measurements taken on the Harshman Bridge. The excellent condition of this bridge, which is over a century old, merits attention and praise, and it serves as an outstanding example of why efforts should be made to conserve the engineering landmarks of our past.